

N92-10120

## Chapter 4

### Impact of Non-Geostationary Orbits on PASS

Dr. Polly Estabrook and Masoud Motamedi

#### 4.1 Introduction

This chapter examines the use of satellites in non-geostationary orbits (NGO) for PASS. This work was undertaken in an effort to investigate alternative system designs to enhance the user capacity and/or reduce the system complexity. The system impact on parameters such as uplink and downlink carrier-to-noise ratios, roundtrip signal delay, Doppler shift, and reduction in satellite antenna size, is quantized for satellites in five circular non-geostationary orbits whose altitudes range from over 20,000 km to under 1,000 km and two elliptical orbits, the Molniya and the ACE orbits. The number of satellites necessary for continuous CONUS coverage and the number of satellite switchovers per day has been determined for the satellites in orbits from 20,000 km to 5,000 km. These higher altitude orbits have been selected for initial study as continental U.S. coverage from one satellite is then possible. Orbits inclinations from the equatorial plane by  $0^\circ$ ,  $45^\circ$ , and  $90^\circ$  have been considered. The increased system complexity brought about by the use of satellites at such altitudes appears to outweigh the system advantages for the application considered in this chapter.

Use of satellites in non-geostationary orbits is motivated by the possibility of gaining the following system advantages: (1) the reduction of EIRP and G/T requirements on the user terminals, thus permitting smaller antenna apertures and smaller terminals, or, equivalently, an increased link margin; (2) lower signal delays through the satellite; (3) reduced satellite antenna size, both for the CONUS and the multiple beam antennas; (4) support of a global communication system, this being especially valid for non-equatorial orbits; and (5) the possibility of using several satellites to operate from higher Earth look angles thus reducing the fade margin and blockage requirements for mobile vehicles applications [1]. Lastly the use of NGO satellites permits the consideration of a greater range of launch vehicles which may permit lower launch costs due to the use of simpler launch vehicles or the launch of

several satellites per vehicle.

While NGOs offer a number of attractive features, there are other factors that must be considered: (1) several satellites will be necessary to provide continuous coverage to any area, hence, control algorithms to handle traffic switchover between satellites must be developed; (2) tracking antennas on Earth will be needed, certainly at the Network Management Center (NMC) and the supplier stations and possibly for the user terminals (although it may be possible to use azimuthally omnidirectional antennas for the latter in some applications [1]); (3) large Doppler shifts will require compensation mechanisms or the design of modulation techniques insensitive to frequency offsets; and (4) variations in link characteristics will occur as the satellite passes from directly overhead to its maximum slant angle. In addition, the design of the satellite will need to cope with radiation effects on the solar panels and electronics due to increased radiation exposure from the Van Allen radiation belt as well as support the more complex antenna pointing mechanisms necessary for non-geostationary operation. Finally, although the use of NGO satellites may alleviate crowding in the geostationary orbit, questions of possible interference between geostationary and NGO satellites must be resolved (see [2] for details).

To date, satellites in non-geostationary circular orbits have been proposed to provide a global mobile communications link at L-band [3]; elliptical orbits have been proposed to offer primary coverage in Europe for mobile users at L-band [1], to offer global coverage for personal and mobile users at Ku band [4], and, to offload traffic from GEO satellites at peak traffic hours for fixed users in the U.S. at C- and Ku-bands [2,5].

This chapter discusses the use of satellites in circular and elliptical orbits; the height of the circular orbits is varied from those at which all of CONUS is visible from the satellite to those at which only parts of CONUS are visible at any one time. All of CONUS is visible with satellites in the two elliptical orbits considered. CONUS coverage from the satellite enables one satellite to relay signals between geographically separated earth stations within CONUS at any one time and thus bypasses the need for intersatellite links (ISL). The three circular orbits from which CONUS coverage is possible have altitudes of 20,182 km, 10,353 km and 5,143 km. For these three orbits, system parameters are found for satellites whose inclination angles from the equatorial plane is  $0^\circ$ ,  $45^\circ$ , and  $90^\circ$ . Similar system parameters are calculated for the two elliptical orbits. In addition the number of satellites required to provide continuous CONUS coverage is calculated for these three higher altitude circular orbits and the two elliptical orbits. System parameters only are given for the two circular orbits at 1,247 km and 879 km that will require ISL to link terminals on either side of CONUS.

The choice of orbit altitudes is explained in Section 4.2. The impact on the uplink and downlink PASS signals is explored in Section 4.3. The calculation of the coverage time provided by satellites in specific locations of a given orbit is delineated in Section 4.4. From this data, the number of satellites required for continuous CONUS coverage is calculated. In Section 4.5 the relative advantages and disadvantages of the use of non-geostationary satellites at these three altitudes are discussed as they relate to the PASS application. Conclusions are presented in Section 4.6.

The material in this chapter has been reported on in [6,7].

## 4.2 Orbit Parameters

Five circular orbits and two elliptical orbits have been chosen for characterization. The heights of the circular orbits vary from that required for geostationary orbit to those easily achievable with a small launch vehicle, such as PEGASUS. Their altitudes therefore span from 20,182 km to 879 km. Two elliptical orbits have been analyzed: the Apogee at Constant time-of-day Equatorial orbit (ACE) studied by Price et al. [2,5]; and the Molniya orbit. Their altitudes vary from 15,100 km to 1030 km for the ACE orbit and from 37,771 km to 426 km for the Molniya orbit.

### 4.2.1 Circular Orbit Characteristics

The heights of the circular orbits have been selected in order to simplify the subsequent calculation of the number of satellites required to provide 24 hr coverage over any chosen area. Satellites heights whose periods are integrally related to the length of one sidereal day,  $\tau_E$ , are considered.<sup>1</sup>

In order to calculate the altitudes of the satellites meeting this constraint, the relationship between satellite period and height must be used. The following equations give the linear velocity of the satellite,  $v_s$ , its angular velocity,  $\omega_s$ , and its period,  $\tau_s$ , in terms of the gravitational constant,  $G$ , the mass of the Earth,  $M$ , the radius of the Earth,  $r_E$ , and the height of the satellite above the Earth,  $h$ :

$$v_s = \sqrt{\frac{G * M}{r_E + h}}, \quad (4.1)$$

$$\omega_s = \frac{v_s}{r_E + h}, \quad (4.2)$$

$$\tau_s = \frac{2\pi}{\omega_s}, \quad (4.3)$$

where

$$G = 6.67 * 10^{-8} \text{ cm}^3/\text{gm sec}^2, \quad (4.4)$$

$$M = 5.976 * 10^{27} \text{ gm}, \quad (4.5)$$

and

$$r_E = 6379.5 \text{ km}.$$

Eqns. 4.1, 4.2, and 4.3 can be used to express  $h$  in terms of  $\tau_s$  :

<sup>1</sup> $\tau_E$  is 23 hrs, 56 min, and 4 sec or 86164 sec.

Table 4.1: Orbital Parameters for Several Circular Orbits

Altitude	Period	$k:n$	$v_s$	$\tau_d$
35,784 km	86164 sec	1:1	11069 km/hr	239 msec
20,182 km	43082 sec	2:1	13946 km/hr	135 msec
10,353 km	21541 sec	4:1	17571 km/hr	69 msec
5,143 km	12309 sec	7:1	21174 km/hr	34 msec
1,247 km	6628 sec	13:1	26027 km/hr	8 msec
879 km	6154 sec	14:1	26678 km/hr	6 msec

$$h = \left( \frac{\tau_s^{\frac{2}{3}} (GM)^{\frac{1}{3}}}{(2\pi)^{\frac{2}{3}}} \right) - r_E \quad (4.6)$$

where we allow  $\tau_s$  to take on only the following values:  $\tau_s = \frac{n}{k} \tau_E$  where  $n$  and  $k$  are integers.

To explore the characteristics of non-geostationary orbits at a variety of altitudes,  $n = 1$  and  $k$  values of 2, 4, 7, 13, and 14 are selected to produce satellite altitudes varying from 20,182 km to 879 km. Satellites can be referred to by the number of times the satellite orbits the Earth in one sidereal day, i.e. their  $k:n$  index. Satellite heights, periods, and velocities for the  $k$  values listed above are given in Table 4.1. Once the satellite height is chosen, then the distance between a point on Earth, viewing the satellite at an elevation angle of  $\phi_l$ , and the satellite can be determined. This distance is known as the slant path  $z$ ; it is shown in Fig. 4.1. The slant path can be calculated according to:

$$z = \sqrt{(r_E \sin \phi_l)^2 + 2r_E h + h^2} - r_E \sin \phi_l. \quad (4.7)$$

The roundtrip signal delay can be computed from:

$$\tau_d = \frac{d}{c} \quad (4.8)$$

where  $c$  is the speed of light,  $3 \cdot 10^5$  km/sec and  $d$  is the distance from transmitting user to satellite to the receiving station. This distance can vary from  $2h$ , when the satellite is directly over the transmitter and receiver, to  $2z$ , when both transmitter and receiver see the satellite at its maximum slant path.  $\tau_d$  is shown in Table 4.1 for  $d = 2h$ .

1/1

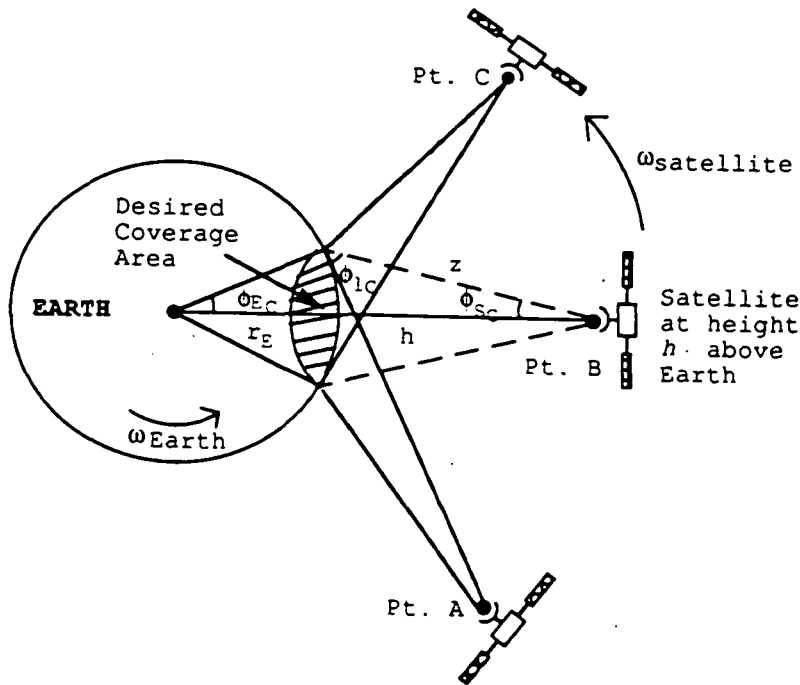


Figure 4.1: Satellite and earth station geometry for satellites in circular orbits.

### 4.2.2 Elliptical Orbit Characteristics

The ACE orbit is an elliptical equatorial orbit with five revolutions per day. It is sun-synchronous and highly eccentric (eccentricity = 0.49). The satellite is at the same point in its arc at the same time each day. The selected orbit has its apogee and perigee at altitudes of 15,100 km and 1,030 km, respectively. The Molniya orbit is a highly elliptical orbit at an inclination of 63.4°. With a perigee of 426 km and an apogee of 37,771 km, the satellite spends most of its orbital period ascending to its apogee. The maximum coverage period for CONUS is attained when its apogee is placed over the center of CONUS.

The following equations relate the period of the satellite's elliptical orbit around the Earth and the satellite velocity to the orbit's geometry:

$$\tau_s = \frac{2\pi a^{\frac{3}{2}}}{\sqrt{G * M}} \quad (4.9)$$

where  $G$  and  $M$  are defined in eqns. 4.4 and 4.5, respectively, and  $a$  is the major semiaxis of the ellipse.  $a$  is equal to one half of the sum of apogee and perigee;

$$v_s = \left[ 2G * M \left( \frac{1}{r_E + h} - \frac{1}{2a} \right) \right]^{\frac{1}{2}} \quad (4.10)$$

where  $r_E$  and  $h$  are defined above. Table 4.2 gives the period, velocity and roundtrip signal delay when satellites in the ACE and Molniya orbits are at their apogee.

Table 4.2: Characteristics of the ACE and Molniya Orbits

Orbit	Altitude	Period	$v_s$	$\tau_d$
ACE	15,100 km	4.8 hrs	11152 km/hr	252 msec
Molniya	39,771 km	12 hrs	5590 km/hr	100 msec

## 4.3 Link Characteristics

### 4.3.1 Doppler Shift

The Doppler shift of the signal is proportional to the velocity vector of the satellite relative to the Earth's motion. Specifically it is proportional to the component of this relative velocity vector which lies in the direction of the receiving earth station,  $v_{relin}$ . The Doppler shift,  $f_{Doppler}$ , can be written as:

$$f_{Doppler} = \pm \left( \frac{v_{relin}}{c} f_c \right) \quad (4.11)$$

where  $c$  is the speed of light and  $f_c$  is the signal frequency. To determine the Doppler shift,  $v_{relin}$  must be found from the angular velocity of the satellite, the inclination angle of the satellite's orbit with respect to the Equator, and the angle between the satellite and the user terminal on Earth.

When  $\phi_l$  and  $\Psi$  are both zero, the Doppler shift can be calculated from the familiar expression:

$$f_{Doppler} = (\omega_E - \omega_s) r_E \frac{f_c}{c}.$$

For orbits with  $\Psi = 0$  the maximum Doppler shift occurs when  $\phi_l = 0$ . These Doppler shifts are given in Table 4.3 at the PASS system uplink frequency of 30 GHz and at the downlink frequency of 20 GHz for a geostationary satellite and for the five circular orbits under consideration.

In order to determine the Doppler shift for satellites in circular orbits with non-zero inclination angles and for satellites in elliptical orbits, the relative velocity between the receiving earth station and the satellite must be found in terms of the satellite velocity vector, the velocity vector of that point on Earth, and the vector between the satellite and the receiving earth station. The following gives a synopsis of the necessary analysis to derive  $v_{relin}$ .

The velocities and locations of a satellite and an earth station can each be decomposed in terms of their three orthogonal components in the geocentric equatorial coordinate system. The origin of this coordinate system is the center of the Earth, its  $x$ -axis points towards the

Table 4.3: Maximum Doppler Shifts for Circular Orbits with  $\Psi = 0$  and  $\Psi = 45^\circ$ .

Altitude	$\Psi = 0$		$\Psi = 45^\circ$	
	30 GHz	20 GHz	30 GHz	20 GHz
35,784 km (GEO)	0.0 KHz	0.0 KHz	0.0 KHz	0.0 KHz
20,182 km	46.5 KHz	31.0 KHz	131 KHz	87 KHz
10,353 km	139.6 KHz	93.0 KHz	216 KHz	144 KHz
5,143 km	279.1 KHz	186.1 KHz	344 KHz	229 KHz
1,247 km	558.2 KHz	372.2 KHz	493 KHz	329 KHz
879 km	604.8 KHz	403.2 KHz	510 KHz	340 KHz

Sun and the  $z$ -axis coincides with the Earth's axis of rotation. The velocity vector,  $\vec{v}_E$ , of an earth station at location  $\vec{P}_E$  is:

$$\begin{aligned}\vec{v}_E = & r_E [\sin(\omega t) + \cos(\omega t + \beta)] \cos \theta_l \hat{i} \\ & + r_E [\cos(\omega t) - \cos(\omega t + \beta)] \cos \theta_l \hat{j} \\ & + 0 \hat{k}\end{aligned}\quad (4.12)$$

where  $\omega t$  denotes the angular distance moved in period  $t$  ( $\omega$  being the angular velocity of the Earth),  $\beta$  is the angle from the  $x$ -axis at  $t = 0$ , and  $\theta_l$  is the latitude of the earth station. The position ( $\vec{P}_s$ ) and the velocity ( $\vec{v}_s$ ) of a satellite can be written similarly. They are omitted from the text due to length of their expressions but can be found in [8].

The relative velocity between the earth station and the earth station and the satellite can be written as:

$$\vec{v}_{rel} = \vec{v}_s - \vec{v}_E. \quad (4.13)$$

The vector between the earth station and the satellite is known as  $\vec{P}_{ES}$ . The component of  $\vec{v}_{rel}$  along the unit vector in the direction of  $\vec{P}_{ES}$  sets the Doppler velocity, i.e.

$$v_{rel.in} = \frac{\vec{v}_s \cdot \vec{P}_{ES}}{|\vec{P}_{ES}|} - \frac{\vec{v}_E \cdot \vec{P}_{ES}}{|\vec{P}_{ES}|}. \quad (4.14)$$

The Doppler shift of the carrier frequency,  $f_c$ , can be obtained by finding the velocity and position vectors of the satellite and the earth station. The Doppler shift is zero when

both  $\vec{v}_s$  and  $\vec{v}_E$  are perpendicular to  $P_{ES}$ . For both the ACE and the Molniya orbits, this occurs when the satellite is at its apogee for those earth stations at the same longitude as the satellite. Alternatively, the Doppler shift will be maximized for earth stations directly under the satellite as the satellite ascending to its apogee or descending from it. The maximum Doppler shift at 30 GHz is approximately 300 KHz and 600 KHz for satellites in the ACE and Molniya orbits, respectively. Maximum Doppler shifts for satellites in circular orbits with  $\Psi = 45^\circ$  are given in Table 4.3.

These large Doppler shifts require a compensation mechanism or a modulation scheme capable of tolerating wide deviations. Doppler compensation techniques would be straightforward if all the communications were done by a central station. The central station would use a set algorithm to change the pilot frequencies going to the user terminals and the downlink frequencies to the supplier stations. However in PASS, where users for a given supplier can be located in different beams, frequency tracking and compensation would put a big burden on the Network Management Center (NMC). The NMC would have to keep track of the position (beam number) of all the users and change the inbound and outbound frequencies accordingly. This would require large guardbands and a real time frequency calculation for all of the active users and suppliers of the system. In Appendix A, it is shown that a real time frequency calculation for all of the active users and suppliers of the system is required. In any case, even after the frequency corrections, depending on the position of a user within a beam pattern, there will be a small residual Doppler that will need to be corrected at the receiver.

The method of using a frequency insensitive modulation scheme has been studied by Simon [9]. Although a less sensitive modulation technique has been devised, larger link margins will be necessary as the frequency offset increases.

### 4.3.2 Propagation Loss

The use of NGO satellites at lower than GEO heights will reduce the propagation loss,  $L_P$ , suffered by the uplink and downlink signals.  $L_P$  can be calculated according to:

$$L_P = \left( \frac{4 \pi d}{\lambda_c} \right)^2 \quad (4.15)$$

where  $\lambda_c$  is the wavelength corresponding to the carrier frequency  $f_c$  and  $d$  can vary from  $h$ , the height of the satellite, to  $z$ , the slant path to the satellite.  $L_P$  is listed in Table 4.4 along with the change in propagation loss,  $\Delta L_P$ , as the satellite orbit altitude is decreased from GEO to 879 km for satellites directly located over the user terminal ( $d = h$ ). As the satellite moves with respect to its coverage area, the range and elevation angle from the user terminals and supplier stations to the satellite varies. The ensuing variation in propagation loss is discussed in Section 4.3.5.

The use of elliptical orbits leads to a changing path range between the satellite and the users. Pt. A in Fig. 4.2 depicts the moment at which all of CONUS is visible from the elliptically orbiting satellite. At this point the range from the earth station (at the

Table 4.4: Propagation Loss for Circular and Elliptical Orbits

Altitude $d$	Propagation Loss 30 GHz $\Delta L_P \dagger$	
Circular Orbits:		
35,784 km (GEO)	213.1 dB	0 dB
20,182 km	208.1 dB	5.0 dB
10,353 km	202.3 dB	10.8 dB
5,143 km	196.2 dB	16.8 dB
1,247 km	183.9 dB	29.2 dB
879 km	180.9 dB	32.2 dB
Elliptical Orbits:		
ACE		
15,100 km *	205.5 dB	7.6 dB
Turn-on/Turn-off ‡	192.5 dB	20.6 dB
Molniya		
39,771 km *	214 dB	-0.9 dB
Turn-on/Turn-off ‡	186 dB	27.1 dB

†  $\Delta L_P = L_{P_{GEO}}(h) - L_{P_{NGO}}(h)$  where  $h$  is the distance from the earth station to the satellite when the satellite is overhead.

\* 20° elevation, at apogee, for earth stations in the center of coverage.

‡ 20° elevation, at turn-on, for earth stations at the farthest edge of coverage.

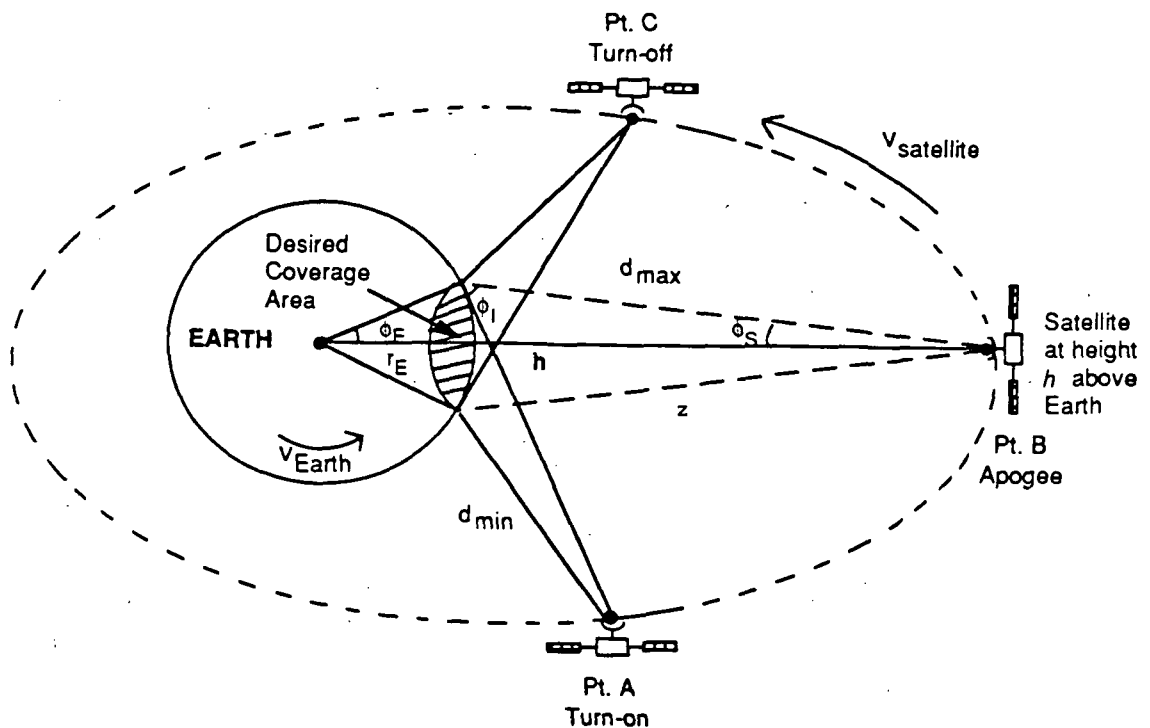


Figure 4.2: Satellite and earth station geometry for satellites in elliptical orbits.

closest edge of coverage) to the satellite,  $d_{min}$ , sets the minimum propagation loss. Pt. B depicts the satellite at its apogee; at this point the range from the earth station (at the farthest edge of coverage) to the satellite,  $d_{max}$ , sets the maximum propagation loss. Pt. C depicts the satellite at the last moment at which all of CONUS is visible. The propagation loss along with its variation compared to GEO is shown in Table 4.4. For the ACE orbit, the improvement in the path loss ranges from 7.6 dB to 20.6 dB. For the Molniya orbit, propagation loss increases relative to GEO by 0.9 dB at orbit apogee.

### 4.3.3 CONUS Coverage Antenna

The preliminary PASS system design utilizes two CONUS beam antennas on the satellite for all communication between the supplier and the satellite. The size of the receive antenna is 0.1m and that of the transmit antenna is 0.15m; both have a gain of 26.9 dBi. In order to determine the effect of operating with NGO satellites, the gain of a CONUS covering antenna is calculated for satellites at various heights  $h$ . The satellite is assumed to have a tracking antenna which is trained on CONUS whenever the latter is visible. This scheme is illustrated in Fig. 4.1. As the satellite moves from Pt. A through Pt. B to Pt. C, the antenna tracks CONUS. Antenna gain is calculated when the satellite is over the middle of

the U.S., i.e. Pt. B in Fig. 4.1.<sup>2</sup>

Antenna gain can be written as:

$$G_{ant} = \rho \frac{4\pi h^2}{2\pi h^2(1 - \cos \phi_S)}, \quad (4.16)$$

where the numerator represents the surface area of a sphere of radius  $h$  and the denominator is the surface area into which the radiated power is directed and  $\rho$  is the aperture efficiency. The satellite then illuminates the area shown by the hatched lines in Fig. 4.1. For CONUS coverage,  $\phi_S$ ,  $\phi_I$ , and  $\phi_E$  in Fig. 4.1 are denoted by  $\phi_{SC}$ ,  $\phi_{IC}$ , and  $\phi_{EC}$ , respectively.  $\phi_{IC}$  is then the minimum elevation angle required for CONUS coverage.

Using the relation  $\frac{\sin \phi_S}{r_E} = \frac{\sin(90 + \phi_I)}{r_E + h}$ ,  $\phi_{SC}$  can be expressed in terms of the minimum elevation angle on Earth to the satellite from:

$$\phi_{SC} = 90^\circ - \cos^{-1} \left( \frac{r_E \cos \phi_{IC}}{r_E + h} \right). \quad (4.17)$$

To find the minimum elevation angle necessary to see a satellite of height  $h$  from CONUS, six points on the perimeter of CONUS are defined. They are listed in Table 4.5. The elevation angle,  $\phi_I$ , is calculated for each location by determining the angle between that location and the satellite. This angle,  $\theta_{ES}$ , is shown in Fig. B.1 in Appendix B where the calculation of  $\phi_I$  and  $\theta_{ES}$  for any point and a satellite at any position is given.

Here we calculate the gain of a CONUS antenna specifically for the case of a satellite in an inclined orbit such that it passes over the center of the US, i.e. its latitude is  $40^\circ$  N and its longitude is  $95^\circ$  W. Satellites in the inclined orbits under consideration will have optimal CONUS coverage at this point. Satellites in equatorial orbits will, of course, never pass over a latitude of  $40^\circ$  N but will have optimal coverage when their longitude is  $95^\circ$  W; the gain of their CONUS antennas will at that point be slightly greater than that of their inclined orbit counterpart as the antenna beamwidth will be slightly narrower.

Once the elevation angles are calculated for each of the locations in Table 4.5, then  $\phi_{IC}$ , or the minimum value of  $\phi_I$ , can be found.  $\phi_{SC}$  can then be calculated from Eq. 4.17 and the gain of a CONUS antenna can be found from Eq. 4.16.

$\phi_{IC}$ ,  $\phi_{SC}$  and CONUS antenna gain  $G_C$  (for  $\rho = 0.5$ ) are given in Table 4.6;  $\phi_{EC}$  is not given as it does not vary with the satellite's height. The minimum CONUS elevation angle,  $\phi_{IC}$ , for a satellite at 35,784 km (equivalent to the height of a geostationary satellite) can be seen from Table 4.6 to be  $64^\circ$ .<sup>3</sup>

In Table 4.6 the 0-3 dB power beamwidth of the CONUS antenna,  $\phi_{SC}$ , increases from  $3.8^\circ$  to  $60.7^\circ$  and the gain of the CONUS antenna falls from 26.6 dB to 2.9 dB as the satellite

<sup>2</sup>Antenna gain for an equatorial orbit could be slightly larger as the beamwidth required to see CONUS from the Equator is less than that required when the satellite is directly over the center of CONUS.

<sup>3</sup>This angle should not be confused with the much lower  $25^\circ$  minimum earth station (E/S) elevation angle required to see a geostationary satellite located in the equatorial arc. A  $25^\circ$  or higher elevation angle is needed for the E/S within CONUS to see a satellite at  $0^\circ$  latitude,  $95^\circ$  longitude, and a height of 35,784 km.

Table 4.5: Cities Considered to Bound CONUS

City	Latitude	Longitude
Bay of Fundy, Maine	47.2°	-68.0°
Key Largo, Florida	25.0°	-80.5°
Brownsville, Texas	26.0°	-97.0°
San Diego, California	32.5°	-117.0°
Seattle, Washington	49.0°	-123.3°
Bottineau, North Dakota	49.0°	-100.0°
Center of USA	40.0°	-95.0°

Table 4.6: Satellite CONUS Antenna Characteristics

Altitude	CONUS Satellite Antenna			
	$\phi_{IC}$	$\phi_{SC}$	$G_{C _{\rho=0.5}}$	$\Delta G_C^\dagger$
Circular Orbits:				
35,784 km	64°	3.8°	26.6 dB	0 dB
20,182 km	61°	6.7°	21.7 dB	-4.9 dB
10,353 km	55°	12.6°	16.2 dB	-10.4 dB
5,143 km	45°	23.0°	11.0 dB	-15.6 dB
1,247 km	13°	54.6°	3.8 dB	-22.8 dB
879 km	7°	60.7°	2.9 dB	-23.7 dB
Elliptical Orbits:				
15,100 km (ACE)	57°	9.3°	19.1 dB	-7.5 dB
39,771 km (Molniya)	65°	3.4°	27.5 dB	+0.6 dB

$$^\dagger \Delta G_C = G_{CNGO} - G_{CGEO}$$

altitude  $h$  is decreased from 35,784 km to 879 km for the circular orbits. The 0-3 dB power beamwidth of the CONUS antenna increases from  $3.8^\circ$  for GEO to  $6.7^\circ$  for the ACE orbit and decreases slightly to  $3.6^\circ$  for the Molniya orbit. The change in CONUS antenna gain relative to a geostationary satellite,  $\Delta G_C$ , is given in the table.

The CONUS antenna size reduction with decreasing gain can be found from the commonly known expression relating antenna gain to antenna area,  $A$  ( $G_{ant} = \rho 4\pi/\lambda^2 A$ ). The antenna diameter,  $d_{ant}$ , can be written as:

$$d_{ant} = \sqrt{\frac{G_{ant}}{\rho}} \cdot \frac{\lambda_c}{\pi}. \quad (4.18)$$

As the satellite altitude drops from 35,784 km (GEO orbit) to 20,182 km, the antenna diameter decreases 43% from 14.4cm to 8.2cm at 20 GHz. The reduction in antenna diameter relative to that required for GEO orbit at 20 GHz is 70%, 83%, 92.8%, and 93.5%, for NGO satellite altitudes of 10,353km ( $d_{ant} = 4.35$ cm), 5,143km ( $d_{ant} = 2.3$ cm), 1,247km ( $d_{ant} = 1.04$ cm), and 879km ( $d_{ant} = 0.94$ cm), respectively. When the ACE orbit is used the required CONUS antenna diameter is 6.1cm (58% reduction); when the Molniya orbit is utilized the required antenna diameter is slightly larger than that necessary for GEO, 16.0cm vs. 14.4cm (size increase of 11%).

#### 4.3.4 Multibeam Antenna Gain

As currently envisaged, the PASS satellite uses two multibeam antennas (MBAs) for communication between the user terminals and the satellite. Each MBA has a beamwidth of  $0.35^\circ$  and uses an 142 beam feed network to cover CONUS. In the preliminary PASS design, the gain of both the transmit and receive MBAs is 52.5 dBi and their efficiencies are both taken to be 0.45, corresponding to a reflector diameter of 2m at 30GHz and 3m at 20GHz. As the satellite orbit height decreases, the spot beams must continue to cover the same area in CONUS. Therefore the required MBA beamwidth will increase from  $0.35^\circ$  and the gain of the MBA will decrease with decreasing satellite altitude.

The impact on antenna beamwidth and gain can be found by equating the GEO and NGO satellite multibeam antenna coverage areas,  $A_{cov}$ , given by the denominator of Eq. 4.16:

$$A_{covGEO} = 2\pi h_{GEO}^2 (1 - \cos \phi_{SMBAGEO}) \quad (4.19)$$

and

$$A_{covNGO} = 2\pi h_{NGO}^2 (1 - \cos \phi_{SMBANGO}) \quad (4.20)$$

where  $\phi_{SMBAGEO}$  is the half-angle subtended from the GEO satellite and  $\phi_{SMBANGO}$  is that subtended from the NGO satellite (refer to Fig. 4.1 for illustration).  $\phi_{SMBANGO}$  can be then found from Eq. 4.19 and 4.20 to be:

$$\phi_{SMBANGO} = \cos^{-1} \left( 1 - \left( \frac{h_{GEO}}{h_{NGO}} \right)^2 (1 - \cos \phi_{SMBAGEO}) \right).$$

Table 4.7: Satellite Multibeam Antenna Characteristics

Altitude	$G_{MBA}$ ( $\rho = 0.45$ )	$\Delta G_{MBA}^\dagger$	$d_{ant}$ (at 20GHz)	Size Change
For circular orbits:				
35,784 km	52.5 dBi	0 dB	3.0 m	0
20,182 km	47.5 dBi	-5.0 dB	1.7 m	43.6%
10,353 km	41.7 dBi	-10.8 dB	86.8 cm	71.1%
5,143 km	35.6 dBi	-16.8 dB	43.1 cm	85.6%
1,247 km	23.3 dBi	-29.2 dB	10.5 cm	96.5%
879 km	20.3 dBi	-32.2 dB	7.4 cm	97.5%
For elliptical orbits:				
15,100 km	45.0 dBi	-7.5 dB	1.3 m	57.7%
39,771 km	53.4 dBi	+0.9 dB	3.3 m	-11.1%

$$^\dagger \Delta G_{MBA} = G_{MBA_{NGO}} - G_{MBA_{GEO}} \text{ (in dB).}$$

The gain of the MBA on the NGO satellite can be found from Eq. 4.16, 4.19, 4.20 assuming that the aperture efficiencies of the NGO antenna and the GEO antenna are equivalent. Written in terms of the ratio of satellite heights,  $G_{MBA_{NGO}}$  becomes:

$$G_{MBA_{NGO}} = \rho \frac{4\pi h_{NGO}^2}{A_{cov_{NGO}}} = \left( \frac{h_{NGO}}{h_{GEO}} \right)^2 G_{MBA_{GEO}}; \quad (4.21)$$

written in terms of the subtended coverage angles,  $G_{MBA_{NGO}}$  becomes:

$$G_{MBA_{NGO}} = \left( \frac{1 - \cos \phi_{SGEO}}{1 - \cos \phi_{SNGO}} \right) G_{MBA_{GEO}}. \quad (4.22)$$

Antenna diameter for these MBAs can be calculated from Eq. 4.18. The ensuing size reduction when compared to GEO operation can then be found. Table 4.7 gives the gain of the MBA antenna and the gain penalty paid for the use of NGO satellites. The size of the MBA at 20 GHz and the size reduction benefit obtained by their use are also tabulated.

#### 4.3.5 Impact on Link Equations

The PASS system is asymmetrical: the user terminal equipment, designed to be handheld and/or portable, is less powerful than the supplier station, a fixed E/S with a 4m antenna. In the communication link from the supplier to the user terminal, the downlink carrier-to-noise ratio sets the overall  $C/N$ . In the link from the user terminal to the supplier, the uplink  $C/N$  sets the overall  $C/N$ . Thus, in both cases the link between the user terminal and the satellite determines the overall quality of the link. In the subsequent discussion  $C/N_{up}$  refers to the uplink  $C/N$  from the user terminal to the satellite, and  $C/N_{down}$  refers to the downlink  $C/N$

151

from the satellite to the user terminal. Both links utilize the satellite's MBAs. In addition  $\Delta C/N_{up}$  refers to the change in  $C/N_{up}$  and  $\Delta C/N_{down}$  refers to the change in  $C/N_{down}$  when the NGO satellite is used in place of the GEO satellite.

Degradation in either  $C/N_{up}$  or  $C/N_{down}$  will require more satellite power and lower satellite receiving temperature.<sup>4</sup> Use of better user equipment (higher gain antenna, higher transmit power, or lower receive temperature) is undesirable as it would increase the terminal's size and power consumption.

Eq. 4.23 gives the relationship between the carrier-to-noise ratio received at the satellite,  $\frac{C}{N_{o_{up}}}$ , the uplink propagation loss, and the satellite's receive MBA gain,  $G_{MBA_r}$ :

$$\frac{C}{N_{o_{up}}} = EIRP_E - L_{P_{up}} + G_{MBA_r} - T_{S_r} - L_{V_{up}} - k \text{ dB-Hz} \quad (4.23)$$

where  $EIRP_E$  is the EIRP of the transmitting E/S,  $T_{S_r}$  is the satellite receiver noise temperature,  $k$  is Boltzmann's constant (-228.6 dBW/K-Hz), and,  $L_{V_{up}}$  is the sum of several losses such as antenna pointing losses, clear sky atmospheric loss, and polarization losses. Eq. 4.24 gives the relationship between the carrier-to-noise ratio received at the E/S,  $\frac{C}{N_{o_{down}}}$ , the downlink propagation loss,  $L_{P_{down}}$ , and the satellite's transmit MBA gain,  $G_{MBA_t}$ :

$$\frac{C}{N_{o_{down}}} = P_{T_s} + G_{MBA_t} - L_{P_{down}} + \frac{G}{T_E} - L_{V_{down}} - k \text{ dB-Hz} \quad (4.24)$$

where  $P_{T_s}$  is the satellite's transmit power and  $\frac{G}{T_E}$  is the  $G/T$  of the receiving E/S and  $L_{V_{down}}$  is the sum of miscellaneous downlink losses. These equations show that reductions in  $L_{P_{up}}$  or  $L_{P_{down}}$  from the use of NGO satellites rather than geostationary satellites (GEO) translate into improvements in the  $\frac{C}{N}$  achievable while reductions in satellite antenna gain translate into degradation of  $\frac{C}{N}$ . The change in uplink  $C/N$  as a consequence of NGO satellites can be written as:

$$\Delta \frac{C}{N_{up}} = (G_{MBA_r_{NGO}} - G_{MBA_r_{GEO}}) + (L_{P_{up_{GEO}}} - L_{P_{up_{NGO}}}). \quad (4.25)$$

The change in downlink  $C/N$  can be written as:

$$\Delta \frac{C}{N_{down}} = (G_{MBA_t_{NGO}} - G_{MBA_t_{GEO}}) + (L_{P_{down_{GEO}}} - L_{P_{down_{NGO}}}). \quad (4.26)$$

To arrive at a worst case estimate of  $\Delta C/N_{up}$  and  $\Delta C/N_{down}$  when the NGO satellite is used, the improvement in propagation loss,  $\Delta L_{P_2}$ , will be evaluated when both satellites are at their maximum slant path from the E/S given the minimum E/S elevation angle allowable.  $\Delta L_{P_2}$  can be found from Eq. 4.15 where  $d$  is the slant path distance  $z$ .  $z$  is calculated from Eq. 4.7 for a particular  $\phi_l$ .  $\Delta L_{P_2}$  is then found to be:

$$\Delta L_{P_2} = \left( \frac{z_{GEO}}{z_{NGO}} \right)^2.$$

<sup>4</sup>Satellite antenna gain can not be changed as it is set by the antenna coverage area.

$\Delta L_{P_2}$  is, of course, frequency independent.

$\Delta L_{P_2}$  is in general less than  $\Delta L_P$  listed in Table 4.4 as the latter tabulates the propagation loss improvement when both satellites are directly overhead. When the NGO satellite is directly overhead,  $\Delta L_{P_2}$  is 0.76 dB higher than  $\Delta L_P$  as the GEO satellite is still considered to be at its maximum slant path.

The change in MBA gain when the NGO satellite is used,  $\Delta G_{MBA}$ , can be found from Eq. 4.21 or 4.22. It is equal to the ratio of the GEO to NGO satellite height when the satellite is overhead:

$$\Delta G_{MBA} = \frac{G_{MBA_{NGO}}}{G_{MBA_{GEO}}} = \left( \frac{h_{NGO}}{h_{GEO}} \right)^2$$

$\Delta G_{MBA}$  is given in Table 4.7. As both the change in propagation loss and in-antenna gain are independent of frequency, Eq. 4.25 and 4.26 can be written as:

$$\Delta \frac{C}{N} = \left( \frac{h_{NGO}}{h_{GEO}} \right)^2 \left( \frac{z_{GEO}}{z_{NGO}} \right)^2 \quad (4.27)$$

$\Delta C/N$  is the change in link margin arising from the use of NGO satellites. It can be calculated from Eq. 4.27 taking  $z_{geo}$  to be the slant path for earth stations with elevation angles of  $25^\circ$  ( $z_{geo} = 39070$  km).  $\Delta C/N$  can also be found from:

$$\Delta C/N = \Delta G_{MBA} + \Delta L_{P_2}$$

where  $\Delta G_{MBA}$  is given in Table 4.7 and  $\Delta L_{P_2}$  is given in Table 4.8.  $\Delta C/N$  is listed in Table 4.8 as  $z_{NGO}$  is varied from its maximum value (when the E/S elevation angle is at  $10^\circ$ ) to its minimum value (when the satellite is directly overhead, i.e.  $\phi_l = 90^\circ$ ).  $\Delta C/N$  will be negative, representing a degradation in  $C/N$ , whenever  $z_{NGO} > h_{NGO} \left( \frac{z_{GEO}}{h_{GEO}} \right)$ .<sup>5</sup>  $\Delta C/N$  will be positive, representing an improvement in  $C/N$ , when the satellite is directly over the E/S.  $\Delta C/N$  will then be  $\left( \frac{z_{GEO}}{h_{GEO}} \right)^2$  or 0.76 dB. This is the maximum improvement in link margin that can be obtained from an NGO satellite assuming that both NGO and GEO satellites must illuminate the same region on Earth, that the antenna efficiencies,  $\rho$ , are equal, and, that identical space and ground segment components are used with both systems.

Table 4.8 also lists the slant path  $z$  and the propagation loss improvement  $\Delta L_{P_2}$  as a function of E/S elevation angle  $\phi_l$ . As the satellite moves accross the sky, the elevation angle required at the E/S varies from the minimum  $\phi_l$  at which the system is operational, for example  $10^\circ$ , to  $90^\circ$  and back to  $10^\circ$ . For an NGO satellite at 20,182 km,  $\Delta C/N$  varies from -0.99 dB to +0.76 dB and back to -0.99 dB. This variation in  $\Delta C/N$  reflects the path loss difference as the satellite moves into and out-of-view from the user terminals and the supplier station. The variation will cause signal level changes that need to be compensated. In the PASS design where it is envisioned that a variable rate modem will be used to compensate for fades due to rain and snow, a new variable will have to be added to the algorithm. This variable, which is a function of time, will provide the means of distinguishing between a true fade and a change in the path loss.

<sup>5</sup>  $z_{GEO}$  is the slant path at  $\phi_l = 25^\circ$  or 39,070 km and  $h_{GEO}$  is 35,784 km.  $\frac{z_{GEO}}{h_{GEO}}$  is then 1.09.

Table 4.8: Link Characteristics for Several Circular Orbits

$\phi_l$	Slant Path $z$	Prop. Loss $\Delta L_{P_2} \dagger$	Link Margin $\Delta C/N$
Altitude = 35,784 km (GEO); MBA Gain = 52.5 dBi			
25°	39070 km	0 dB	
Altitude = 20,182 km; MBA Gain = 47.5 dBi			
10°	24700 km	3.98 dB	-0.99 dB
20°	23694 km	4.34 dB	-0.63 dB
30°	22791 km	4.68 dB	-0.29 dB
90°	20182 km	5.74 dB	+0.76 dB
Altitude = 10,353 km; MBA Gain = 41.7 dBi			
10°	14401 km	8.67 dB	-2.10 dB
20°	13440 km	9.27 dB	-1.50 dB
30°	12605 km	9.83 dB	-0.94 dB
90°	10353 km	11.54 dB	+0.76 dB
Altitude = 5,143 km; MBA Gain = 35.6 dBi			
10°	8551 km	13.20 dB	-3.65 dB
20°	7658 km	14.15 dB	-2.70 dB
30°	6922 km	15.03 dB	-1.82 dB
90°	5143 km	17.61 dB	+0.76 dB
Altitude = 1,247 km; MBA Gain = 23.3 dBi			
10°	3215 km	21.69 dB	-7.47 dB
20°	2532 km	23.77 dB	-5.39 dB
30°	2067 km	25.53 dB	-3.63 dB
90°	1247 km	29.92 dB	+0.76 dB
Altitude = 879 km; MBA Gain = 20.3 dBi			
10°	2528 km	23.78 dB	-8.41 dB
20°	1911 km	26.21 dB	-5.98 dB
30°	1518 km	28.21 dB	-3.98 dB
90°	879 km	32.96 dB	+0.76 dB

$\dagger \Delta L_{P_2} = L_P(z)_{GEO} - L_P(z)_{NGO}$  where  $z$  is the maximum slant path for a given  $\phi_l$ .

## 4.4 Number of Satellites Required for Continuous CONUS Coverage

### 4.4.1 Circular Orbit Results

In order to compute the number of satellites necessary to provide 24 hr coverage of a particular region, the start and stop times at which the satellite is visible from all points within that coverage area must be calculated. This coverage time,  $T_{cc}$ , depends on the minimum elevation angle,  $\phi_{l_{min}}$ , that the earth stations in the coverage area are permitted to operate with.  $T_{cc}$  is also a function of the initial angular position,  $\theta_S$ , of the satellite in its orbit. Given a particular orbit, coverage area and  $\phi_{l_{min}}$ ,  $T_{cc}$  and its corresponding start and stop times are calculated for satellite initial angular positions ranging from  $0^\circ$  to  $360^\circ$ . Then a reasonable set of satellite locations can be selected to maximize CONUS coverage. Continuous CONUS coverage generally requires the use of satellites in several orbit planes, all identically inclined from the equator. Satellites in each of these orbit planes are then chosen so that the start and stop times of each satellite overlap to provide 24 hr coverage of the coverage area in question. The number of satellites required for continuous area coverage is then computed from the number of satellites used in each of the identically inclined orbits. These steps are detailed below.

Calculation of the start and stop times for CONUS coverage for satellites in circular orbits at any inclination from the equator is performed with the aid of the program *eleangle.f*. In order to minimize computational time, only orbits whose period have an integer relationship to the Earth rotational period are considered, i.e.  $T_{satellite} = n/k T_{earth}$  where  $n$  and  $k$  are integers. For the orbits described in Table 4.1,  $n = 1$  and  $k$  is 2, 4, 7, 13 and 14. Satellites in these orbits will appear over the same spot on the Earth each day.

The program calculates the trajectory of the satellite as a function of time. Points on Earth are assumed to move relative to a Sun fixed coordinate system. This coordinate system has as its origin the center of the Earth; it is denoted in rectangular coordinates as  $x$ ,  $y$ , and  $z$  where  $z = 0$  specifies the equatorial plane of the Earth. Points on the surface of the Earth are specified by their longitude and latitude in the  $x$ ,  $y$ ,  $z$  coordinate system. As the surface of the Earth turns about this coordinate system, the longitudes of these points vary  $360^\circ$  from their Earth-prescribed values but their latitudes remain constant. Seven points within CONUS are chosen for the calculation: six cities on the perimeter of CONUS and one located roughly in the middle of the U.S.. The longitude and latitude of the points are shown in Table 4.5. The motion of any of these locations is described in Cartesian coordinates as:

$$\begin{aligned} x_{loc}(t) &= r_E \sin \phi \cos(\omega_E t + \theta), \\ y_{loc}(t) &= r_E \sin \phi \sin(\omega_E t + \theta), \\ z_{loc}(t) &= r_E \cos \phi, \end{aligned} \quad (4.28)$$

where the latitude and longitude of the terrestrial location are related to  $\phi$  ( $\phi = 90^\circ - \text{latitude}$ ) and  $\theta$  ( $\theta = \text{longitude}$ ), respectively.

A second coordinate system,  $x'$ ,  $y'$ , and  $z'$ , is used to describe the motion of the satellite. Its  $x' - z'$  plane is inclined from the  $x - z$  plane by  $\Psi$ , the inclination angle of the satellite's orbit relative to the equatorial plane. The center of this coordinate system is also the center of the Earth; hence the centers of the two coordinate systems are co-located. In the  $x'$ ,  $y'$ , and  $z'$  system, the satellite traces a circle whose radius is  $h + r_E$ :

$$\begin{aligned}x'_{sat}(t) &= (h + r_E) \cos(\omega_{sat}t + \theta_S), \\y'_{sat}(t) &= (h + r_E) \sin(\omega_{sat}t + \theta_S), \\z'_{sat}(t) &= 0,\end{aligned}$$

where  $h$  is the height of the satellite above the Earth,  $\omega_{sat}$  is the angular velocity of the satellite and  $\theta_S$  is the starting position of the satellite at  $t = 0$ . The satellite motion can be translated to the  $x$ ,  $y$ , and  $z$  coordinate system according to:

$$\begin{aligned}x_{sat}(t) &= \cos \Psi x'_{sat}(t) - \sin \Psi z'_{sat}(t), \\y_{sat}(t) &= y'_{sat}(t), \\z_{sat}(t) &= -\sin \Psi x'_{sat}(t) + \cos \Psi z'_{sat}(t),\end{aligned}$$

or,

$$\begin{aligned}x_{sat}(t) &= (h + r_E) \cos \Psi \cos(\omega_{sat}t + \theta_S), \\y_{sat}(t) &= (h + r_E) \sin(\omega_{sat}t + \theta_S), \\z_{sat}(t) &= -(h + r_E) \sin \Psi \cos(\omega_{sat}t + \theta_S).\end{aligned}\tag{4.29}$$

The program finds the elevation angle,  $\phi_l$ , from the seven points listed in Table 4.5 to the satellite for one satellite period according to Eq. B.4 in Appendix B. At the end of this period, the satellite's position relative to the points on CONUS is identical to that at the beginning of the calculation because of the integer relationship between Earth rotation period and satellite period.

The start and stop of each city's coverage period during one Earth day is determined by the times at which  $\phi_l \geq \phi_{l_{min}}$ . The start time for a CONUS coverage period is found by determining the time at which all seven points have elevation angles just greater than  $\phi_{l_{min}}$  to the satellite. The end time is determined by the time interval before the elevation angle at one of the seven points falls below  $\phi_{l_{min}}$ .

Use of the program enables study of the number of satellites required vs. orbit height, orbit inclination angle, and minimum elevation angle. To illustrate the type of output it generates and to characterize the effect of inclination angle on the NGO satellite system, performance with satellites at an altitude of 20,182 km at three orbital inclination angles,  $\Psi = 0^\circ$ ,  $45^\circ$ , and  $90^\circ$ , will be detailed. The sequence of steps performed to calculate the number of satellites and their location necessary to provide continuous CONUS coverage is outlined in Figure 4.3.

1. For each orbit under consideration, find the orbit period  $\tau_s$ , decide upon the appropriate time increment, e.g.  $\frac{\tau_s}{100}$ , and calculate time steps:  $t(k) = (k - 1) \frac{\tau_s}{100}$ .
2. The latitude and longitude of each of the 7 points in CONUS listed in Table 4.5 is used along with  $t(k)$  to find the motion of these points (relative to the center of the Earth) as a function of time: i.e.  $x_{loc1}(t(k))$ ,  $y_{loc1}(t(k))$ , and  $z_{loc1}(t(k))$  are found using Eq. 4.28.
3. For a given initial satellite position,  $\theta_S$ , find  $x_{loc1}(t(k))$ ,  $y_{loc1}(t(k))$ , and  $z_{loc1}(t(k))$  from Eq. 4.29.
4. At each time increment  $t(k)$  find the elevation angle between each location and the satellite i.e.  $\phi_{loc1}(t(k))$ ,  $\phi_{loc2}(t(k))$ ,  $\dots$ ,  $\phi_{loc7}(t(k))$  from Eq. B.4 in Appendix B
5. Do steps 2. - 4. for  $t(k) = 0$  to  $\tau_s$ .
6. Find the start and stop times ( $T_{start}(1)$ ,  $T_{stop}(1)$ ) of each time window such that:

$$\begin{aligned}
 \phi_{loc1}(t(k)) &\geq \phi_{l_{min}} \\
 \phi_{loc2}(t(k)) &\geq \phi_{l_{min}} \\
 &\vdots \\
 \phi_{loc7}(t(k)) &\geq \phi_{l_{min}}.
 \end{aligned}$$

For satellites in inclined orbits, there may be more than 1 time window per day at which all of CONUS is visible. Denote the number of these time windows per day as  $i$ .

7. Perform steps 2. - 6. for satellites with initial angular positions in their orbit  $\theta_S$  varying from  $0^\circ$  to  $360^\circ$ .
8. Plot  $T_{start}(i)$  and  $T_{stop}(i)$  for each of the  $i$  windows vs. the satellite initial angular position  $\theta_S$ , e.g. see Fig. 4.5, 4.8, and 4.11.
9. From the above figure determine the set of optimum  $\theta_S$ ,  $\{\theta_{S_{opt}}\}$ , to get 24 hr CONUS coverage with the fewest satellites.

If 24 hr coverage is not possible using satellites in this orbit plane only, then create another  $\theta_S$  vs.  $T_{cc}$  pattern shifted in time to provide additional coverage. See Fig. 4.9 and 4.12 for examples.

Figure 4.3: Steps performed in the calculation of the number and the location of satellites required to provide continual CONUS coverage.

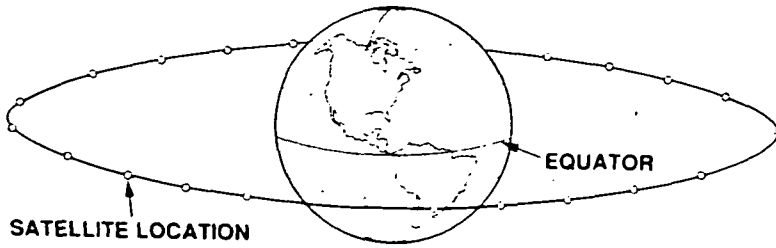


Figure 4.4: Satellite location for equatorial orbit.

#### Satellite orbit at 20,182 km, inclination angle at $0^\circ$

The first example concerns an equatorial circular orbit at 20,182 km ( $k:n = 2:1$ ). The characteristics of this orbit are shown in Tables 4.1, 4.3 and 4.4. The program is run to find the complete coverage window for all seven cities assuming that at  $t = 0$  the satellite at  $\theta_s = 0^\circ$  is at longitude  $= 0^\circ$ .  $\theta_s$  is varied in steps of  $11.125^\circ$ . The orbit and the satellites are shown in Fig. 4.4. The program results are given in Fig. 4.5. Note that each satellite, equally positioned around the orbital arc, sees CONUS once for the same amount of time during one Earth day.<sup>6</sup> The start and stop times of  $T_{cc}$  depend on the initial position of the satellite with respect to CONUS at  $t = 0$ . The program is run with  $\Delta t = 95$  sec. Two values of  $\phi_{l_{min}}$  are considered:  $\phi_{l_{min}} = 10^\circ$  and  $\phi_{l_{min}} = 20^\circ$ .  $T_{cc}$  is 3:20 hrs for the former and 0:58 hrs for the latter. Because  $T_{cc}$  does not depend on satellite location in the orbital arc, the number of satellites,  $N_{satellite}$ , can easily be calculated according to:

$$N_{satellite} = \text{Integer} \left\{ \frac{24 \text{ hrs}}{T_{cc} + T_{overlap}} \right\} \quad (4.30)$$

where  $T_{overlap}$  is the amount of overlap desired between satellites and *Integer* is a function which rounds its argument up to produce an integer value.  $N_{satellite}$  is then found to be:

$$N_{sat} = \begin{cases} 8 & \text{for } \phi_{l_{min}} = 10^\circ \\ 25 & \text{for } \phi_{l_{min}} = 20^\circ \end{cases} \quad (4.31)$$

Fig. 4.6 gives the angular location of the 8 satellites needed to provide CONUS coverage for  $\phi_{l_{min}} = 10^\circ$ .

<sup>6</sup>The satellite sees CONUS once a day although it passes over the location where CONUS was twice in one day. In other words, let us assume that at  $t = 0$  CONUS is visible to the satellite. This will be the case again at  $t = 23\text{hrs } 56\text{min and } 4\text{sec}$ . At  $t \approx 12$  hrs, the satellite will pass over the point in the fixed coordinate system where CONUS was but CONUS will now have moved halfway around the globe and be invisible to the satellite.

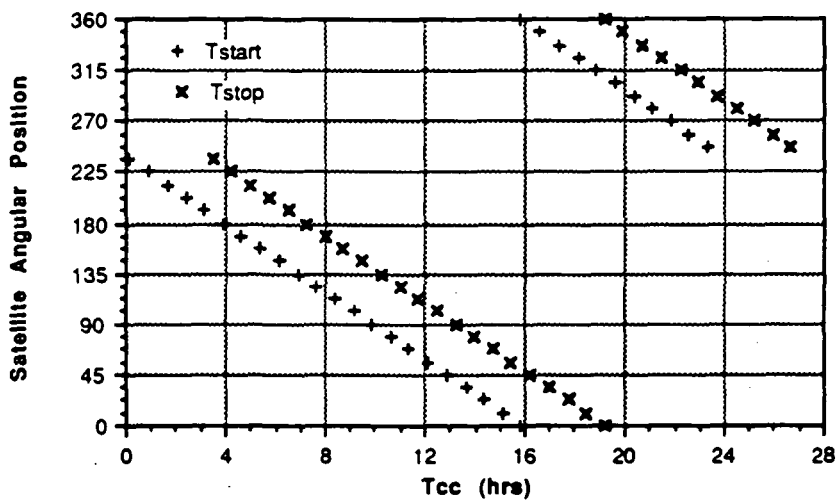


Figure 4.5:  $T_{cc}$  for each satellite  $11.125^\circ$  apart in an equatorial orbit at 20,182 km for  $\phi_{l_{min}} = 10^\circ$ .

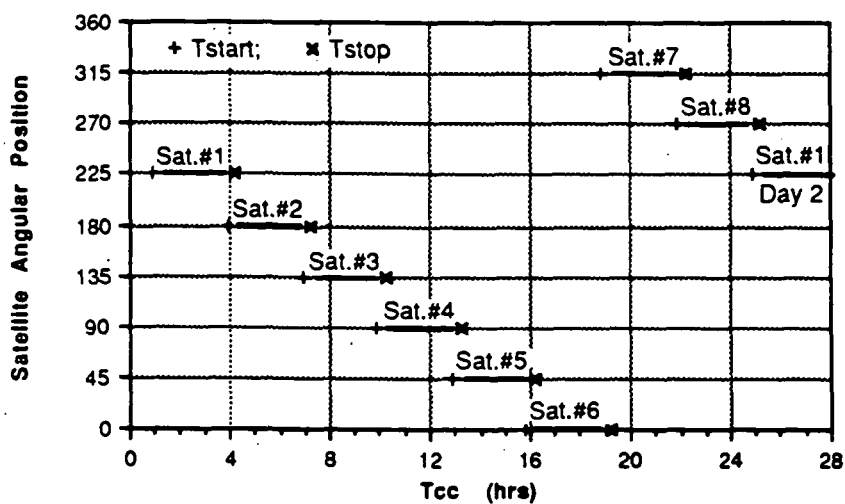


Figure 4.6: Location of the eight satellites necessary for complete CONUS coverage: equatorial orbit at an altitude of 20,182 km;  $\phi_{l_{min}} = 10^\circ$ .

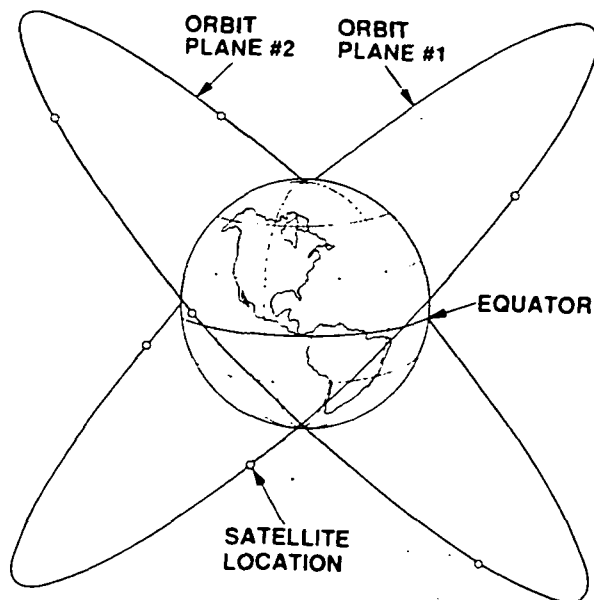


Figure 4.7: Satellite location for a circular orbit at an inclination angle of  $45^\circ$ .

#### Satellite orbit at 20,182 km, inclination angle at $45^\circ$

The performance of a circular 20,182 km orbit inclined from the equator by  $45^\circ$  is now found. Of course there are many such orbits that can be placed about the globe. Two are depicted in Fig. 4.7; they can be uniquely identified by their longitude at the equator at the time  $t = 0$ . The two depicted differ by  $180^\circ$ . The coverage times,  $T_{cc}$ , have been calculated for satellites spaced  $11.125^\circ$  apart in orbit #1; they are shown in Fig. 4.8. Again, the satellite sees CONUS only once every day, i.e. one coverage window per day. However, contrary to the equatorial orbit case, it is immediately apparent that  $T_{cc}$  depends on the satellite's angular position at  $t = 0$ . For  $\theta_s$  from  $135^\circ$  to  $225^\circ$ , the satellite sees CONUS for very small time periods. This can be understood by examining Fig. 4.7: although satellites in this orbit will cross the longitudes corresponding to CONUS once per day and thus might be expected to be visible to CONUS, in fact some satellites will cross these longitudes when they are in the southern hemisphere and thus barely visible to CONUS. (No CONUS coverage is feasible for satellites at these angular positions when  $\phi_{l_{min}} = 20^\circ$ .)

Examination of Fig. 4.8 shows that continuous CONUS coverage is not possible if satellites are placed only in this  $45^\circ$  orbit as no coverage is available from  $t = 0$  hrs to  $t = 0.5$  hrs and from  $t \approx 16$  hrs to  $t = 24$  hrs. If the  $T_{cc}$  coverage pattern can be shifted in time by 12 hrs, corresponding to angular difference in the  $45^\circ$  orbit of  $180^\circ$ , then continuous CONUS coverage can be achieved. The ensuing  $T_{cc}$  pattern is shown in Fig. 4.9. Orbits #1 and #2 differ only in their relative position to the Earth at  $t = 0$ . The relative position of CONUS and orbit #1 at  $t = 0$  is identical to that of CONUS and orbit #2 12 hours later. To find the coverage pattern provided by satellites located in any  $45^\circ$  orbit, it is sufficient to calculate the  $T_{cc}$  obtained vs.  $\theta_s$  for a specific  $45^\circ$  orbit and then shift the time axis of that pattern by  $t$  hours to arrive at the  $T_{cc}$  pattern of an orbit  $t/24 \cdot 360^\circ$  away.

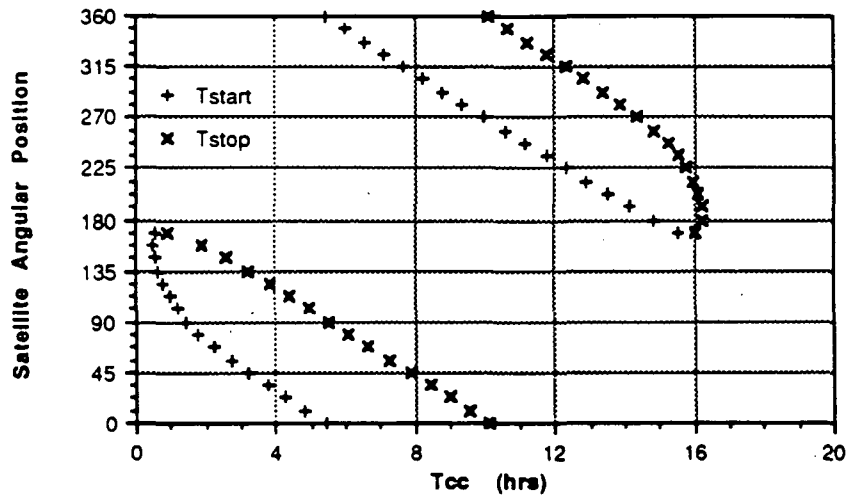


Figure 4.8:  $T_{cc}$  for each satellite  $11.125^\circ$  apart in a 20,182 km orbit inclined by  $45^\circ$  for  $\phi_{e,min} = 10^\circ$ .

Examination of Fig. 4.9 shows that 24 hr CONUS coverage can be achieved by choosing the appropriate initial angular positions for satellites in each of the  $45^\circ$  orbits. Because  $T_{cc}$  varies for each  $\theta_S$ , the optimum satellite positions must be determined graphically. Choosing  $\theta_S$  so as to maximize  $T_{cc}$ , three satellites can be placed at  $\theta_S = 90^\circ, 0^\circ$ , and  $270^\circ$  in orbit #1 to provide greater than 12 hr coverage. Three satellites can be located at  $\theta_S = 78.75^\circ, 348.75^\circ$ , and  $270^\circ$  in orbit #2 to provide the remaining 12 hrs of coverage. These six satellites are shown in Fig. 4.9. Thus six satellites are necessary with one coverage window per satellite per day. The number of coverage windows per day,  $N_{window}$ , is then six.  $N_{window}$  is a measure of the tradeoff complexity that will be necessary to handle the daily handoffs between satellites.

The average  $T_{cc}$ ,  $\langle T_{cc,system} \rangle$ , of these six satellites can be computed from the coverage time of each of these windows according to:

$$\langle T_{cc,system} \rangle = \frac{\sum_{N_w=1}^{N_{windows}} T_{cc}}{N_{windows}} \quad (4.32)$$

For this example,  $\langle T_{cc,system} \rangle$  is calculated to be 4hrs 26min. The overlap time between satellites can be found from:

$$\text{Overlap} = \frac{\sum_{N_w=1}^{N_{windows}} T_{cc} - 24\text{hrs}}{24\text{hrs}} \quad (4.33)$$

In this case the overlap is computed to be 11%.

For  $\phi_{l,min}$  of  $20^\circ$ , 8 satellites, 4 in each orbit, will suffice to provide continuous CONUS coverage with 16.8% overlap between satellites.  $\langle T_{cc,system} \rangle$  is 3hrs 30 min.

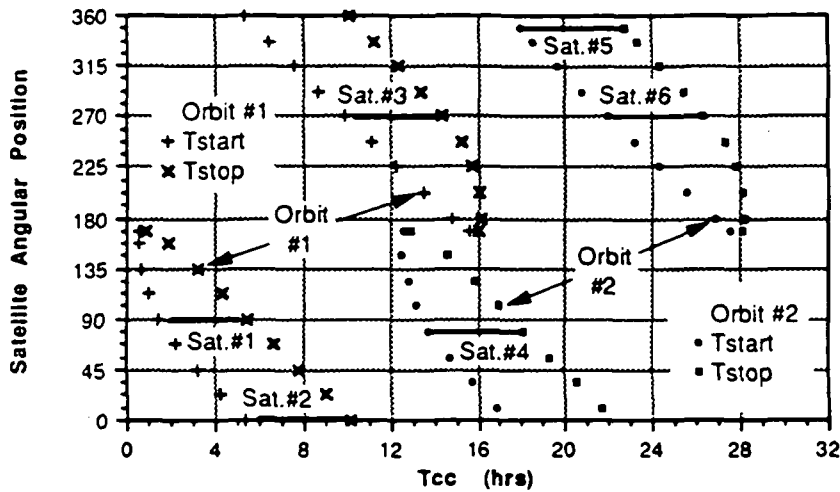


Figure 4.9: Satellite location in two 45° inclined 20,182 km orbits to provide continuous CONUS coverage assuming  $\phi_{l_{min}} = 10^\circ$ .

#### Satellite orbit at 20,182 km, inclination angle at 90°

When satellite orbits at inclination angles of 90° are used, more satellites are necessary to achieve 24 hr coverage. Fig. 4.10 illustrates the case of two polar orbits separated by 97.5° – a minimum satellite geometry for  $\phi_{l_{min}}$  is 10°. The coverage times for satellites in a 90° orbit are shown in Fig. 4.11 for  $\phi_{l_{min}} = 10^\circ$ . For the majority of satellite angular positions, there are two coverage windows per day. However for  $\theta_s$  from 56.25° to 45°, only one coverage window exists per day. In either case, the coverage period per window is very short. As with the 45° inclination angle orbits, it is necessary to place satellites in two orbits in order to provide continuous CONUS coverage. The optimum phase difference between these orbits must be determined by trial and error so as to select satellites in both orbits to provide 24 hr coverage. A possible solution to minimize the number of satellites required is given in Fig. 4.12. The two orbits differ by 6.5 hrs or 97.5°. Seven satellites, 4 in orbit #1 and 3 in orbit #2, are required. Satellites #1, #2, #3, and #5 are used twice each day. (The second coverage window of the satellite is drawn with a hatched pattern.) The number of coverage windows per day for continuous CONUS coverage,  $N_{window}$ , is then 11, meaning that a transceiver operating continuously would have to perform 11 satellite handoffs per day.

$\langle T_{cc,system} \rangle$  can be calculated from Eq. 4.32 to be 2hrs 46min and the overlap can be found from Eq. 4.33 to be 26.7%.

For  $\phi_{l_{min}} = 20^\circ$ , 3 satellite orbits are necessary; they are separated by 60°.  $N_{satellite}$  is 9,  $N_{window}$  is 14,  $\langle T_{cc,system} \rangle$  is 2 hrs 9min, and there is 26% overlap between satellites.

The results for use of NGO satellites in a circular orbit at 20,182 km for orbit inclination angles of 0°, 45°, and 90° are shown in Table 4.9. Note that an inclination angle of 45° permits use of the smallest number of satellites and the fewest number of satellite handoffs

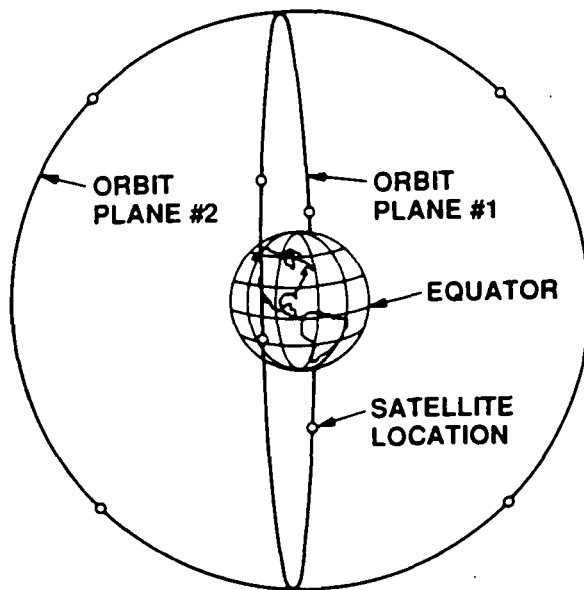


Figure 4.10: Satellite locations for two circular orbits at an inclination angle of  $90^\circ$ .

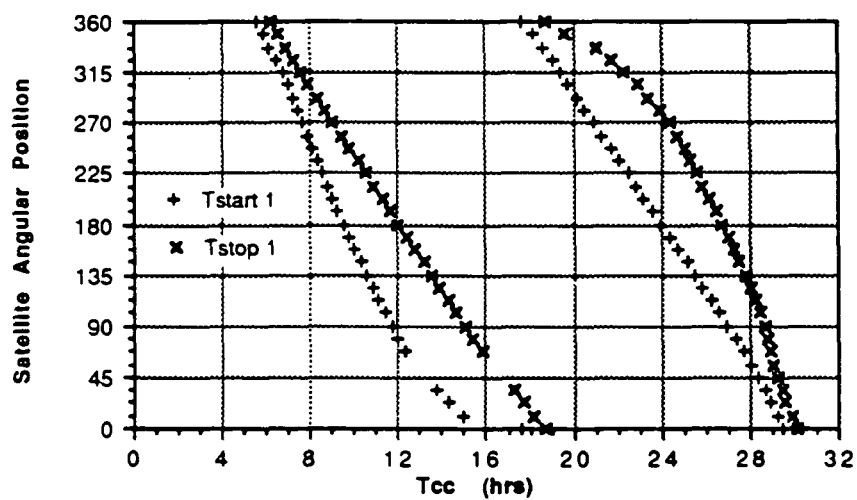


Figure 4.11:  $T_{cc}$  for each satellite  $11.125^\circ$  apart in a 20,182 km orbit inclined at  $90^\circ$  for  $\phi_{lmin} = 10^\circ$ .

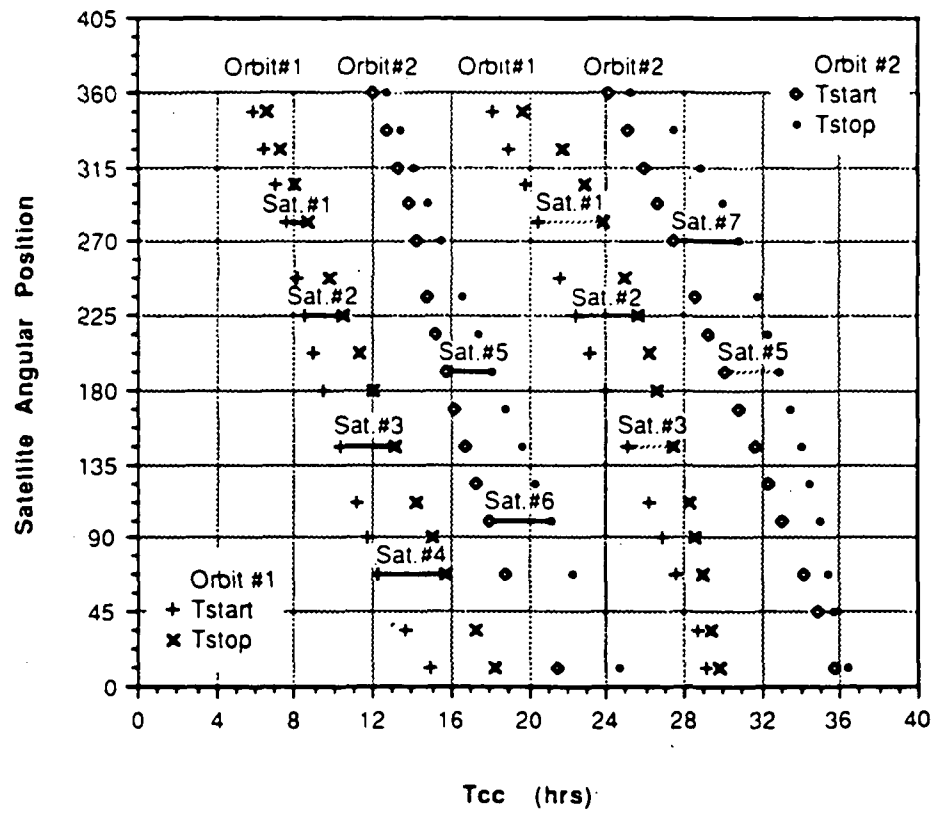


Figure 4.12: Satellite location in two  $90^\circ$  inclined 20,182 km orbits to provide continuous CONUS coverage assuming  $\phi_{l_{min}} = 10^\circ$ .

Table 4.9: Satellite Orbit Parameters for Circular Orbits at a Height of 20,182 km for Various Inclination Angles,  $\Psi$ , and Min. Elevation Angle,  $\phi_{l_{min}}$

	$\Psi = 0^\circ$		$\Psi = 45^\circ$		$\Psi = 90^\circ$	
	$\phi_{l_{min}} = 10^\circ$	$\phi_{l_{min}} = 20^\circ$	$\phi_{l_{min}} = 10^\circ$	$\phi_{l_{min}} = 20^\circ$	$\phi_{l_{min}} = 10^\circ$	$\phi_{l_{min}} = 20^\circ$
$N_{satellite}$	8	25	6	8	7	9
Orbit Planes	1 plane	1 plane	2 planes	2 planes	2 planes	3 planes
$\Delta\theta_{orbit}$	N/A †	N/A	$0^\circ, 180^\circ$	$0^\circ, 180^\circ$	$0^\circ, 97.5^\circ$	$0^\circ, 60^\circ, 120^\circ$
$N_{coverage}$	8	25	6	8	11	14
$\langle T_{cc_{system}} \rangle$	3hrs 20min	59min	4hrs 26min	3hrs 30min	2hrs 46min	2hrs 9min
$N_{window}$	1	1	1	0, 1	1, 2	0, 2
Overlap	11.4%	2.5%	11.0%	16.8%	26.7%	26.0%

† Not Applicable.

per day.

#### Satellite orbit at 10,353 km, inclination angle at $0^\circ$ , $45^\circ$ , and $90^\circ$

The characteristics of NGO satellite systems operating at an altitude of 10,353 km are shown in Table 4.10 for orbit inclination angles of  $0^\circ$  and  $45^\circ$ . Orbit parameters are not shown for satellites in equatorial orbits when  $\phi_{l_{min}}$  is  $20^\circ$  as it is not possible then for the satellite to see all of CONUS no matter what its initial angular position is. Although certain portions of the US are visible with elevation angles greater than  $20^\circ$ , at no time do all seven points chosen to represent the boundaries of CONUS have elevation angles greater than  $20^\circ$ . The overall effect of a reduction in satellite altitude by a factor of 2 is to reduce  $\langle T_{cc_{system}} \rangle$  by a factor of 3 to 4 so that, even though the number of satellites does not triple, the number of satellite handoffs per day does.

#### Satellite orbit at 5,143 km, inclination angle at $0^\circ$ , $45^\circ$ , and $90^\circ$

The characteristics of NGO satellite systems operating at an altitude of 5,143 km are shown in Table 4.11 for orbit inclination angles of  $45^\circ$  as satellites in equatorial orbits cannot provide CONUS coverage when  $\phi_{l_{min}}$  is greater than  $10^\circ$ . The number of satellites required is now 26 for  $\phi_{l_{min}} \leq 10^\circ$  and 48 for  $\phi_{l_{min}} \leq 20^\circ$ .  $\langle T_{cc_{system}} \rangle$  is 33 min and 23 min for  $\phi_{l_{min}} \leq 10^\circ$  and  $\phi_{l_{min}} \leq 20^\circ$ , respectively. The number of satellite handoffs per day is 56 and 101 for  $\phi_{l_{min}} \leq 10^\circ$  and  $\phi_{l_{min}} \leq 20^\circ$ , respectively.

Table 4.10: Satellite Orbit Parameters for Circular Orbits at a Height of 10,353 km for Various Inclination Angles,  $\Psi$ , and Min. Elevation Angle,  $\phi_{l_{min}}$

	$\Psi = 0^\circ$	$\Psi = 45^\circ$	
	$\phi_{l_{min}} = 10^\circ$	$\phi_{l_{min}} = 10^\circ$	$\phi_{l_{min}} = 20^\circ$
$N_{satellite}$	20	12	18
Orbit Planes	1 plane	2 planes	3 planes
$\Delta\theta_{orbit}$	N/A †	$0^\circ, 180^\circ$	$0^\circ, 120^\circ, 240^\circ$
$N_{coverage}$	60	20	24
$\langle T_{ccsystem} \rangle$	25min	1hrs 28min	1hrs 7min
$N_{window}$	3	2	1, 2
Overlap	3.8%	22.1%	12.3%

† Not Applicable.

Table 4.11: Satellite Orbit Parameters for Circular Orbits at a Height of 5,143 km for an Inclination Angle,  $\Psi$ , of  $45^\circ$  and Two Minimum Elevation Angles,  $\phi_{l_{min}}$

	$\Psi = 45^\circ$	
	$\phi_{l_{min}} = 10^\circ$	$\phi_{l_{min}} = 20^\circ$
$N_{satellite}$	26	48
Orbit Planes	3 planes	3 planes
$\Delta\theta_{orbit}$	$0^\circ, 150^\circ, 300^\circ$	$0^\circ, 132^\circ, 264^\circ$
$N_{coverage}$	56	101
$\langle T_{ccsystem} \rangle$	33 min	23 min
$N_{window}$	3, 4	2, 3
Overlap	28.8%	60.8%

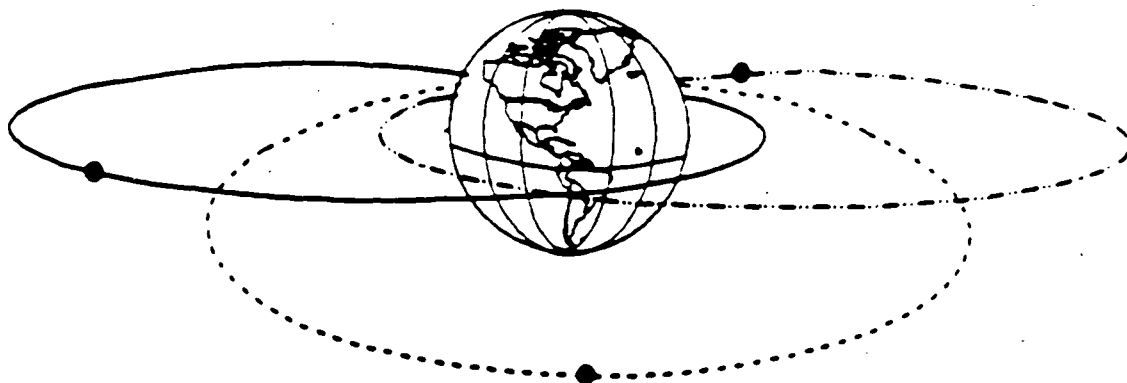


Figure 4.13: Satellite location for three satellites in three ACE orbits.

#### 4.4.2 Elliptical Orbit Results

##### ACE orbit

Approximately eight satellites are required to provide continuous CONUS coverage from this orbit. The total coverage period and thus the number of satellites can be calculated from finding the turn-on and turn-off points of the satellite assuming that the satellite antennas have their boresights directed towards the center of CONUS during the coverage period. As depicted in Fig. 4.13 satellites in the ACE orbit can be phased in order to give a 24hr CONUS coverage. These satellites, with their orbit apogees at  $0^\circ$  latitude and  $-95^\circ$  longitude, would turn their transponders on at the first point that  $\phi_{l_{min}} = 20^\circ$  and turn them off at the next  $\phi_{l_{min}} = 20^\circ$ .

##### Molniya orbit

The satellites in the Molniya orbit are phased in the same fashion as the ACE satellites. Approximately three satellites, with their apogee at  $37^\circ$  latitude and  $-95^\circ$  longitude, are required to provide continuous CONUS coverage from this orbit.

### 4.5 Advantages and Disadvantages of NGOs

The relative advantages and disadvantages to using NGO satellites for the PASS application can be measured in terms of the parameters mentioned in the introduction. This chapter has focused on determining some of them, for instance, the variation in propagation loss during the satellite's pass over CONUS, the impact on the signal uplink and downlink, the roundtrip signal delay, Doppler shift, reduction in the size of satellite antennas, number of satellite switchovers/day and the number of satellites required to cover CONUS continually. These parameters are given in Table 4.12 for the three NGO satellite altitudes at which

CONUS coverage from one satellite is possible and for the two elliptical orbits considered. An inclination angle of  $45^\circ$  is chosen to minimize the number of satellites although the use of non-equatorial orbits does lead to slightly higher maximum Doppler shifts and lower antenna gains.

In Table 4.12  $\Delta L_{P_1}$  represents the variation in propagation loss from the time when the satellite first becomes visible at  $\phi_{l_{min}}$  to the time when the satellite is overhead,  $\phi_{l_{min}} = 90^\circ$ . It is given by  $L_P(z) - L_P(h)$  where  $z$  is the maximum slant path distance and  $h$  is the distance from the satellite to an E/S directly underneath it. It can be calculated from  $\Delta L_{P_2}$  given in Table 4.8; for example  $\Delta L_{P_1}(10^\circ) = \Delta L_{P_2}(90^\circ) - \Delta L_{P_2}(10^\circ)$ . The link margin for the circular orbits is that shown in Table 4.8. For elliptical orbits it is calculated for earth stations within CONUS having the minimum elevation angle: for the Molniya orbit  $\phi_{l_{min}}$  is  $41^\circ$ .  $N_{cov}$  and  $N_{sat}$  are taken from Tables 4.9, 4.10 and 4.11. The round trip delay is taken from Table 4.1 for the circular orbits and Table 4.2 for the elliptical orbits. Doppler shift is shown for circular orbits with  $\Psi = 45^\circ$ ; it is taken from Table 4.3. Doppler shift for the elliptical orbits is taken from Section 4.3.1. Satellite antenna size is given for the CONUS antenna ( $\rho = 0.5$ ) and the MBA antenna ( $\rho = 0.45$ ); these values are taken from Section 4.3.3 and Table 4.7.

As can be seen from Table 4.12, no improvement in the link is achieved with the NGO satellites in circular orbits as long as  $\phi_{l_{min}}$  is  $20^\circ$  or less.<sup>7</sup> The gain in signal power brought about by the reduced propagation loss when NGO satellites are used is outweighed by the loss in satellite antenna gain. For the PASS design, the degradation in uplink  $C/N$  means that both suppliers and users will have to transmit higher EIRPs; the degradation in downlink  $C/N$  will require both suppliers and users to increase their receive  $G/T$ . This most certainly means that the size of the user antenna could not be reduced: directional antennas will still be necessary as in the preliminary design. Moreover the user and supplier antennas will require satellite tracking mechanisms for both circular or elliptical orbits. Both user and supplier transceivers will need to implement techniques to compensate for the Doppler shift of the signal which at 20 GHz and 30 GHz is substantial, up to 344 KHz for satellites in  $45^\circ$  inclined orbits at altitudes of 5,143 km. Lastly the variation in the link will necessitate some modification to the present rain fade control scheme wherein both users and suppliers utilize the signal strength of the pilot to determine the rain fade condition in their uplink and downlink.

A comparison of the orbits under consideration shows that the fewest number of satellites required for continual CONUS coverage is the Molniya orbit which requires only three. It also requires the smallest change in link margin when compared to the geostationary orbit. However this orbit has the highest maximum Doppler shift and possesses a wide range in path loss. The 20,182 km circular orbit has far less Doppler shift and negligible path loss change with less link margin degradation but requires 6 to 8 satellites depending on  $\phi_{l_{min}}$ . Lower orbits require greater numbers of satellites, have greater degradation in the link margin, possess higher variations in the path loss, and are characterized by higher Doppler shifts;

<sup>7</sup>Consideration of low elevation angles is necessary to maximize  $T_{cc}$  and hence minimize the number of satellite switchovers per day and the number of satellites necessary for continuous CONUS coverage.

Table 4.12: GEO and NGO Satellite Parameter Comparison

Elev. Angle $\phi_{l_{min}}$	Prop. Loss $\Delta L_{P_1}$	Link Margin $\Delta C/N$	$N_{cov.}$	$N_{sat.}$	Roundtrip Delay (Overhead)	Doppler Shift(max) at 30 GHz	Satellite Antenna † at 20 GHz CONUS   MBA	
Circular Orbits								
For 35,784 km (GEO) altitude satellite, $\Psi = 45^\circ$ :								
10°	0	0	1	1	239 msec	0 KHz	14.4cm	3.0m
For 20,182 km altitude satellites, $\Psi = 45^\circ$ :								
10°	1.8 dB	-0.99 dB	6	6	135 msec	131 KHz	8.2cm	1.7m
20°	1.4 dB	-0.63 dB	8	8			(43%)	(44%)
For 10,353 km altitude satellites, $\Psi = 45^\circ$ :								
10°	2.9 dB	-2.1 dB	20	12	69 msec	216 KHz	4.3cm	0.87m
20°	2.3 dB	-1.5 dB	24	18			(70%)	(71%)
For 5,143 km altitude satellites, $\Psi = 45^\circ$ :								
10°	4.4 dB	-3.6 dB	56	26	34 msec	344 KHz	2.3cm	0.43m
20°	3.5 dB	-2.7 dB	101	48			(83%)	(86%)
Elliptical Orbits								
For 15,100 km altitude (ACE) satellites, $\Psi = 0^\circ$ :								
20°	6 dB	-1.7 dB		8	252 msec	300 KHz	6.1cm (58%)	1.3m (58%)
For 39,771 km altitude (Molniya) satellites, $\Psi = 63.4^\circ$ :								
41°‡	5 dB	-0.4 dB		3	100 msec	600 KHz	16.0cm (-11%)	3.3m (-11%)

† Reduction in antenna size compared to GEO is given in parenthesis.

‡ The minimum elevation angle for earth stations within CONUS with the Molniya satellite is 41°.

167

however they have greater advantages in terms of signal delay and reduction in satellite antenna size.

Independent of the orbit, the benefits of using NGO satellites for this system are the reduced roundtrip signal delay and reduced satellite antenna size. The latter is of particular importance for the transmit and receive multibeam antennas where a size reduction of 16% to 79% is possible for satellite heights from 20,182 km to 5,143 km. This weight reduction in the communication payload may be offset by the more sophisticated antenna pointing mechanism required for the MBAs and by the larger solar cells, battery size, or electrical shielding which may be necessary to protect against the increased radiation found in these orbits. For satellite altitudes of 20,182 km and 10,353 km, the number of satellites and number of satellite switchovers per day are manageable.

Other advantages arising from the use of NGO satellites mentioned in the introduction, such as the possibility of global communications or improvements in the radio channel for mobile users, are not applicable to the PASS system as it is currently defined.

## 4.6 Conclusion

This chapter has studied the effects on the link characteristics of satellite in five circular non-geostationary orbits whose altitudes range from over 20,000 km to under 1,000 km and two elliptical orbits. The number of satellites necessary for continuous CONUS coverage and the number of satellite switchovers per day has been determined for the satellites in circular orbits from 20,000 km to 5,000 km as these altitudes allow CONUS to be covered by one satellite and for satellites in each of the elliptical orbits. Lower satellite altitudes require the use of more than one satellite and intersatellite links between satellites to provide CONUS coverage at any one time. The relative advantages and disadvantages of using NGO satellites for the PASS application are measured in terms of the following parameters: the impact on the signal uplink and downlink, the roundtrip signal delay, Doppler shift, reduction in the size of satellite antennas, number of satellite switchovers/day and the number of satellites required to cover CONUS continually.

The advantages of using satellites in circular orbits at altitudes ranging from 20,000 km to 5,000 km or in the ACE and Molniya elliptical orbits do not appear to outweigh the increased system complexity for the Personal Communication Satellite System application considered in this chapter. This is due, in large part, to this application's requirement to support real-time interactive voice between users located anywhere within CONUS. This requirement constrains the amount of time that the satellite can be used to be equal to the CONUS coverage time for high altitude satellites and sets the requirement for intersatellite links if lower altitude satellites are used. Greater system benefits might be realizable for this latter case. Such satellites would, however, require intersatellite links to maintain system interconnectivity. They will necessitate signal processing and routing functions on-board the satellite which may dramatically increase its cost and weight to values comparable to geostationary satellites.

## Appendix A

# Implication of Doppler Shift on the Complexity of the Channel Assignment Routine

To a stationary observer, the frequency of a moving transmitter varies with the transmitter's velocity. If a stationary transmitter's frequency is at  $f_T$ , the received frequency  $f_R$  is higher than  $f_T$  when the transmitter is moving toward the receiver and lower than  $f_T$  when the transmitter is moving away from the receiver. This change in frequency, or Doppler shift, is quite pronounced for low orbiting satellites and compensating for it requires intense frequency assignment and tracking.

For a non-geosynchronous satellite system linking supplier stations to users scattered around CONUS, direct supervision of the frequency assignment by a network management routine is required. The management routine has to ensure that no two signals in any link overlap, that is for any two signals centered at  $f_n$  and  $f_m$  in a given link,

$$|f_n - f_m| > BW, \quad (\text{A.1})$$

where  $BW$  is the required data bandwidth.

For the PASS forward link, all the suppliers will have to compensate for the Doppler shift by tracking the incoming pilot from the satellite thus ensuring that the same nominal frequency is received by the satellite from all suppliers transmitting via a TDM/TDMA channel to a particular beam.

Denoting the signal destined to beam  $b$  by  $F_{up}(b)$ , onboard the satellite the signal is frequency shifted using a constant frequency  $F_{for}(b)$  and is transmitted using beam  $b$ . This signal  $F_{down}(b)$  received by user  $n$ ,  $U_n$ , is in the form of:

$$F_{down}(b, U_n) = F_{up}(b) + F_{for}(b) + \text{Doppler}(U_n) \quad (\text{A.2})$$

where  $\text{Doppler}(U_n)$  is the Doppler shift due to the motion of the satellite as observed by the  $n^{\text{th}}$  user. The Doppler shift varies from one user to the other as a function of their positions. Following the channel assignment of Eq. A.1 the network controller has to ensure that in an

area where frequency reuse is not implemented, for any beam number  $p$  and  $q$  ( $p \neq q$ ), and  $i$  and  $j$  ( $i \neq j$ ),

$$|F_{down}(p, U_i) - F_{down}(q, U_j)| > BW_{forward}, \quad (A.3)$$

thus requiring wide guard bands or a constant changing of the TDMA channels center frequencies based on the location of the users in communication.

In the return direction where SCPC channels are assigned to users for transmission, the assignment procedure includes selection of an even greater number of center frequencies. In this link, assuming that Doppler correction is done on the inbound channel, means should be taken to correct the transmit frequency so that overlap at the satellite are avoided. That is at the satellite for any  $k$  and  $l$  ( $k \neq l$ ) in a region without frequency reuse:

$$|F_{user_k} - F_{user_l}| > BW_{return}. \quad (A.4)$$

Furthermore, the downlink from the satellite to the suppliers will require frequency correction based on the received pilot by the suppliers.

## Appendix B

# Calculation of the Elevation Angle from an Earth Station $E$ to a Satellite at an Arbitrary Location, $S$ .

For a satellite at a particular latitude, longitude and height, the elevation angle between a point on Earth and the satellite can be determined by taking the dot product between the vector from the center of the Earth to the point on the Earth,  $\vec{E}$ , and the vector from the point on Earth to the satellite,  $\vec{ES}$ :

$$\cos \theta_{ES} = \vec{E} \cdot \vec{ES}. \quad (\text{B.1})$$

The vectors  $\vec{E}$ ,  $\vec{S}$ , and  $\vec{ES}$  and the angle  $\theta_{ES}$  are shown in Figure B.1.  $\vec{E}$ ,  $\vec{S}$ , and  $\vec{ES}$  can be written in terms of the  $x$ ,  $y$ , and  $z$  components of each vector as follows:

$$\begin{aligned} \vec{E} &= E_x \hat{i} + E_y \hat{j} + E_z \hat{k}, \\ \vec{S} &= S_x \hat{i} + S_y \hat{j} + S_z \hat{k}, \\ \vec{ES} &= ES_x \hat{i} + ES_y \hat{j} + ES_z \hat{k}. \end{aligned}$$

$\vec{ES}$  can also be expressed in terms of  $\vec{E}$  and  $\vec{S}$ :

$$\vec{ES} = (S_x - E_x) \hat{i} + (S_y - E_y) \hat{j} + (S_z - E_z) \hat{k}. \quad (\text{B.2})$$

The angle between  $\vec{E}$  and  $\vec{ES}$ ,  $\theta_{ES}$ , can then be found from the definition of the dot product to be:

$$\theta_{ES} = \cos^{-1} \left( \frac{(E_x * (S_x - E_x)) + (E_y * (S_y - E_y)) + (E_z * (S_z - E_z))}{|E| |ES|} \right) \quad (\text{B.3})$$

where  $|E|$  and  $|ES|$  represent the magnitude of  $\vec{E}$  and  $\vec{ES}$ . The elevation angle from the point in CONUS to the satellite is then given by:

$$\phi_I = 90^\circ - \theta_{ES}. \quad (B.4)$$

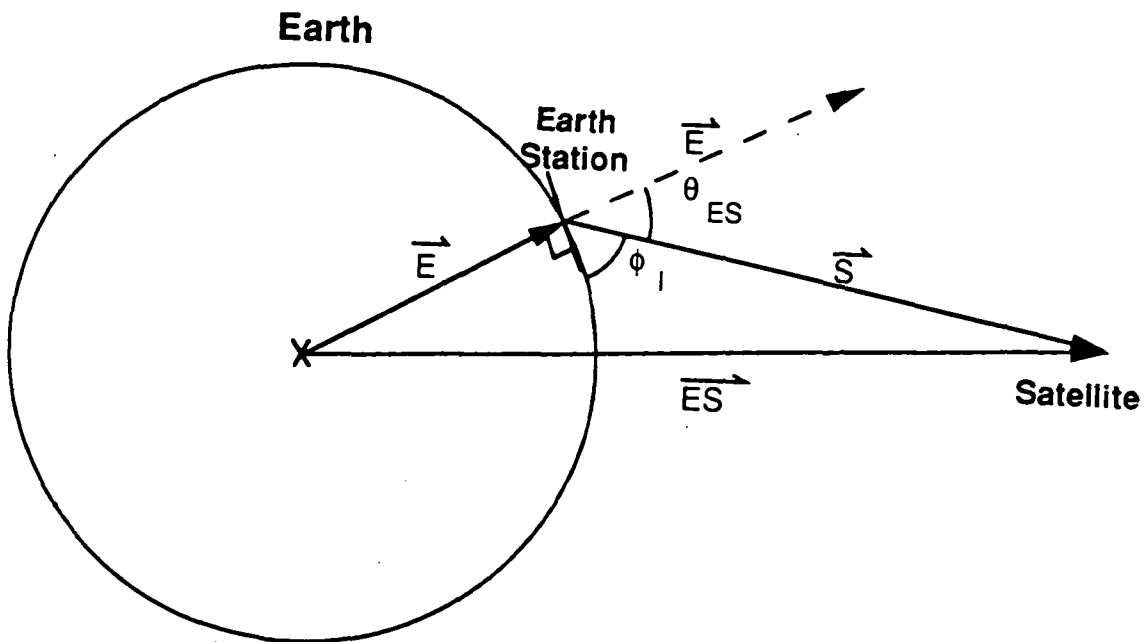


Figure B.1: Elevation angle geometry.

# Bibliography

- [1] Stuart, J.R., Norbury, J.A., and Barton, S.K., *Mobile Satellite Communications from Highly Inclined Elliptic Orbits*, AIAA 12th International Communications Satellite Systems Conference, March 13-17, 1988, Virginia, pg. 535 to 541.
- [2] Price, Kent M., Doong, Wen, Nguyen, Tuan Q., Turner, Andrew E., and Weyandt, Charles, *Communications Satellites in Non-Geostationary Orbits*, AIAA 12th International Communications Satellite Systems Conference, March 13-17, 1988, Virginia, pg. 485 to 495.
- [3] Richharia, M., Hansel, P.H., Bousquet, P.W., and O'Donnell, M., *A Feasibility Study of a Mobile Communication Network using a Constellation of Low Earth Orbit Satellites*, IEEE Global Telecommunications Conference, November 27-30, 1989, Texas, pg. 21.7.1 - 21.7.5.
- [4] Nauck, J., Horn, P., and Göschel, W., - *LOOPUS - MOBILE - D - A New Mobile Communication Satellite System*, AIAA 13th International Communications Satellite Systems Conference, March 11-15, 1990, Los Angeles, California, pg. 886 to 899.
- [5] Ford Aerospace, *The Use of Satellites in Non-Geostationary Orbits for Unloading Geostationary Communications Satellite Traffic Peaks, Volumes I and II*, NASA publication, CR-179-597.
- [6] Estabrook, P. and Motamedi, M., *Use of Non-Geostationary Orbits for a Ka-Band Personal Access Satellite System*, AIAA 13th International Communications Satellite Systems Conference, March 11-15, 1990, Los Angeles, California, pg. 14 to 24.
- [7] Motamedi, M. and Estabrook, P., *Use of Elliptical Orbits for a Ka-Band Personal Access Satellite System*, Second International Mobile Satellite Conference, June 17 - 20, 1990, Ottawa, Canada.
- [8] *Orbital Flight Handbook Part 1 - Basic Techniques and Data*, NASA SP-33 Part 1, National Aero. and Space Admin., Washington, D.C., 1963, pg. III-24.
- [9] Sue, M. (ed), *Personal Access Satellite System Concept Study*, JPL D-5990 (Internal Document), Jet Propulsion Laboratory, February 1989.

- [10] Bousquet, M. and Maral, G., *Orbital Aspects and Useful Relations from Earth Satellite Geometry in the Frame of Future Mobile Satellite Systems*, AIAA 13th International Communications Satellite Systems Conference, March 11-15, 1990, Los Angeles, California, pg. 783 to 789.
- [11] Pratt, Timothy and Bostian, Charles W., *Satellite Communications*, John Wiley & Sons, 1986.